

Breather-induced anomalous charge diffusionG. Kalosakas,¹ K. L. Ngai,² and S. Flach¹¹*Max Planck Institute for the Physics of Complex Systems, Nöthnitzer Strasse 38, Dresden 01187, Germany*²*Naval Research Laboratory, Washington, D.C., 20375-5320, USA*

(Received 8 November 2004; published 3 June 2005)

We present results on the diffusive motion of a charge interacting with the nonlinear dynamics of a thermalized underlying lattice. Signatures of anomalous diffusive properties are found at relatively high temperatures, where highly nonlinear excitations are present. A sublinear diffusion and a plateau appear before the standard long-time diffusion during the evolution of the mean-squared displacement and a significant degree of heterogeneity is exhibited among individual trajectories. Both properties are connected with the existence of vibrational hot spots (breather or multibreather excitations). Transport parameters of the charge are strongly affected in this case, as can be exemplified by the significant suppression of the diffusion coefficient D . The variation of D with temperature follows a stretched exponential law. The results are contrasted with those of the linearized case, in the absence of breathers. Such anomalous diffusion of a charge coupled to a thermalized lattice may be relevant in low-dimensional soft materials with strong anharmonicities, such as biomolecules, conducting polymers, etc.

DOI: 10.1103/PhysRevE.71.061901

PACS number(s): 87.15.-v, 63.22.+m, 05.90.+m

I. INTRODUCTION

The problem of charge transport in low-dimensional flexible materials, apart from its own fundamental interest, is related to important technological or biological issues. For example, many optoelectronic devices have been constructed by conjugated polymers [1], while the potential use of DNA in molecular electronics has attracted considerable attention [2] (for recent reviews on charge transport in DNA see Refs. [3,4]). Furthermore, charge migration along biomolecules may be involved in various biological processes.

In all these cases, the propagating charge interacts with the underlying flexible structure [5–8]. A convenient way to include the effects of intrinsic structural dynamics on charge transport is provided through coupled charge-lattice microscopic dynamical models, which are commonly used for the study of polarons. In this respect, the Su-Schrieffer-Heeger model has been successfully used for the study of organic conductors [5,6,9], while a variety of models have been proposed for the case of DNA [10–13], depending on which parameter of the charge transport (on-site energy or overlap integral) is coupled to the structural motions of the double helix and which intramolecular degrees of freedom are involved in this interaction. The evolution of such coupled systems is easily obtained numerically in the approximation of the semiclassical equations of motion [14]. In this framework, thermal fluctuations can be incorporated by using Langevin dynamics for the classical lattice component [15] [see Eq. (3) below.]

Using this formalism, it has been recently shown that for relatively high temperatures (i.e., when highly anharmonic excitations are present), vibrational hot spots enhance the spatial confinement of a charge carrier, and the dependence of this phenomenon on the temperature and the charge-lattice coupling constant has been investigated [15]. The strong anharmonicity of the lattice is responsible for these hot spots and their presence becomes more evident by increasing temperature. They constitute manifestations of breathers [16,17]

at finite temperatures [18] and their lifetime is orders of magnitude longer than the characteristic time scales of the corresponding normal modes [19].

Here, continuing the study of the effects observed at the microscopic level in Ref. [15], we consider *macroscopic* characteristics of charge transport in a dynamical nonlinear lattice, by examining its diffusive properties. We follow the evolution of the charge's mean-squared displacement and calculate the diffusion coefficient through the long-time linear dependence. We find that hot spots give rise to a sublinear time dependence or a plateau in the mean-squared displacement and a significant degree of heterogeneity among individual trajectories. Such a behavior is reminiscent of anomalous relaxation in glass-forming systems [20–22]. In the latter case, mutual interaction and concomitant caging effects slow down the motion of particles and hinder their diffusion, resulting in a characteristic plateau. In our case, charge's confinement and irregular motion is provided by the thermally induced hot spots in the lattice.

The structure of the paper is as follows. In the next section, we briefly present the dynamical model we use. In Sec. III, the time evolution of the mean-squared displacement is discussed and compared to the corresponding linearized case, in order to clarify the effects of the hot spots. Section IV presents the variation of the diffusion coefficient with temperature, which is also compared to the corresponding results obtained for the linearized case. Section V presents calculations of the non-Gaussian parameter, which quantifies the deviation of the charge probability from a Gaussian shape. Finally, in the last section we draw our conclusions.

II. THE MODEL

We consider the diagonal coupling (on the on-site energies) of a tight-binding charge with the Peyrard-Bishop-Dauxois (PBD) [23] lattice-dynamical model. The Hamiltonian of the charge-lattice interacting system reads

$$\begin{aligned}
H = & -V \sum_n (c_n^\dagger c_{n+1} + c_n^\dagger c_{n-1}) + \chi \sum_n y_n c_n^\dagger c_n \\
& + \sum_n \left[\frac{1}{2} m \dot{y}_n^2 + D(e^{-ay_n} - 1)^2 \right. \\
& \left. + \frac{k}{2} (1 + \rho e^{-\beta(y_n + y_{n-1})}) (y_n - y_{n-1})^2 \right]. \quad (1)
\end{aligned}$$

The index n enumerates the lattice sites on which the charge propagates and c_n^\dagger, c_n are the corresponding creation and annihilation operators. The first term in Eq. (1) is a tight-binding Hamiltonian allowing hopping between adjacent sites with transfer integral V . The second term provides the charge-lattice interaction through the linear coupling of charge's on-site energy with the displacement y_n of the corresponding lattice site (χ is the coupling constant). Finally, the last sum is the PBD Hamiltonian, consisting of the kinetic energy, an on-site Morse potential, and a nonlinear intersite interaction; m is the mass of the oscillators at each lattice site, D and a the parameters of the Morse potential, and k, ρ, β , the parameters of the intersite interactions.

The PBD model has been used to accurately describe the nonlinearities of the stretching vibrations of hydrogen-bond paired bases within a base pair in DNA [23–26] (i.e., the anharmonic dynamics of base pair openings). The interaction of a charge with the PBD model, as given by the Hamiltonian (1), has been introduced in order to study the effects of thermal fluctuations in charge transport in DNA. More details with respect to this description can be found in Refs. [12,15]. Here, we consider the PBD model as representing a typical, breather-bearing, nonlinear lattice. We expect our results to apply in general to charge diffusion on thermalized nonlinear discrete systems, wherever charge-lattice interaction exists and strong lattice anharmonicities are present.

We consider the case of a homogeneous lattice in order to isolate the effects of nonlinearity from static disorder. The site-independent parameter values used are $V=0.1$ eV, $\chi=0.6$ eV/Å, $m=300$ amu, $D=0.04$ eV, $a=4.45$ Å⁻¹, $k=0.04$ eV/Å², $\rho=0.5$, and $\beta=0.35$ Å⁻¹. These values are relevant for the case of DNA apart from the charge-lattice coupling parameter χ , where there is no realistic estimate available. Here, we present results for the value of $\chi=0.6$ eV/Å, which corresponds to a weak coupling, in the sense that a large polaron is the ground state of the system at zero temperature [12]. We note that, using these parameters, an enhanced charge trapping due to vibrational hot spots at the microscopic level has been previously observed [15], which is the motivation of our present calculation of macroscopic diffusion properties.

In the semiclassical approximation [14], supplemented by a Langevin description of the classical component of lattice dynamics, the equations of motion for the charge wave function Ψ_n and the displacements y_n are [15]

$$i\hbar \frac{d\Psi_n}{dt} = -V(\Psi_{n+1} + \Psi_{n-1}) + \chi y_n \Psi_n \quad (2)$$

and

$$\begin{aligned}
m \frac{d^2 y_n}{dt^2} = & -M'(y_n) - W'(y_n, y_{n-1}) - W'(y_{n+1}, y_n) - \chi |\Psi_n|^2 \\
& - m \gamma \frac{dy_n}{dt} + f_n(t), \quad (3)
\end{aligned}$$

where $M(y)$ is the Morse potential and $W(x, y)$ is the intersite interaction [the last two terms, respectively, in Hamiltonian (1)], and a prime denotes differentiation with respect to y_n . For the friction constant in Eq. (3), we have used the value $\gamma=0.005$ ps⁻¹, while the random force $f_n(t)$ has the usual statistical properties: $\langle f_n(t) \rangle = 0$ and $\langle f_n(t) f_{n'}(t') \rangle = 2k_B T m \gamma \delta_{n,n'} \delta(t-t')$, where k_B is the Boltzmann constant and T the temperature. The significant influence of lattice thermal motions in the propagation of the charge is coming through the last term in the Schrödinger equation (2), where the lattice displacements provide fluctuating on-site energies for the charge.

III. ANOMALOUS DIFFUSION DUE TO HOT SPOTS

To investigate diffusive properties of a charge coupled to the nonlinear lattice dynamics, we start with an initial wave function completely localized at the site n_0 ,

$$\Psi_n(t=0) = \delta_{n,n_0}, \quad (4)$$

while the lattice is thermalized at temperature T , and, by solving Eqs. (2) and (3), calculate the evolution of charge's mean-squared displacement

$$x^2(t) = \sum_n (nl)^2 |\Psi_n(t)|^2 - (n_0 l)^2, \quad (5)$$

where l is the lattice constant. The $x^2(t)$ in Eq. (5) is a quantum mean value. Then a thermal average $\langle x^2(t) \rangle$ is obtained over a number of different realizations of the thermalized lattice. Since there is no external bias, the mean value of the charge displacement along the lattice is $\langle x \rangle = n_0 l$.

In Fig. 1, we present the charge's mean-squared displacement as a function of time for various temperatures, ranging from 10 K up to 350 K. In log-log scale, $\langle x^2(t) \rangle$ starts linearly with a slope 2 (i.e., $\langle x^2 \rangle \sim t^2$) for very short times (at fs time scales), while at sufficiently long times (of the order of ps) it acquires a slope 1 (i.e., $\langle x^2 \rangle \sim t$), as it is expected in diffusion [27]. While this crossover is smooth at lower temperatures, at higher T a fractional power-law dependence or sublinear diffusion appears, which becomes a plateau preceding the standard long-time behavior at the highest temperatures. The higher the temperature, the more evident is this anomalous relaxation.

As mentioned in the Introduction, in the microscopic level the distinctive feature of the system at higher temperatures is the appearance of hot spots in lattice dynamics, which result in an enhanced confinement of the charge [15]. In particular, charge is found to be trapped between hot spots (see Fig. 5 of Ref. [15]) up to ps time scales. The higher the temperature, the higher the intensity of hot spots. The existence of hot spots is responsible for the anomalous behavior revealed in the $\langle x^2(t) \rangle$ dependence in Fig. 1. To demonstrate that indeed

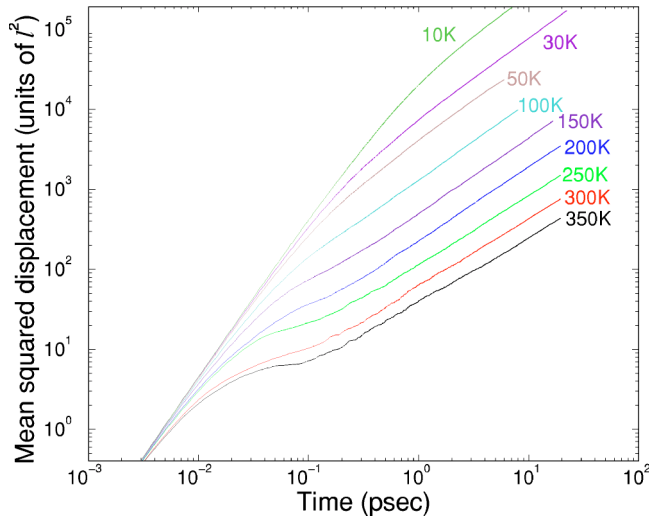


FIG. 1. (Color online) Time dependence of the mean-squared displacement $\langle x^2(t) \rangle$ (in units of squared lattice constant l^2), averaged over 200 thermal realizations, for different temperatures. The size of the system varies from 500 up to a few thousands of lattice sites, depending on the temperature (the lower the T , the larger the size of the system). Parameter values are given in the text.

this is the case, we have performed similar calculations by changing key components in the lattice PBD Hamiltonian of the system. Results for the mean-squared displacement have been obtained for three different situations: (i) the full Hamiltonian (1), (ii) by switching off the nonlinearity only in the intersite interaction, i.e., putting $\rho=0$, while keeping the Morse on-site potential, and (iii) in the completely linearized problem with $\rho=0$ and substitution of the Morse potential by its linearized form $M_{\text{lin}}(y_n) = Da^2 y_n^2$. In cases (i) and (ii), there

exist hot spots at high temperatures, while they are absent in the linearized case (iii). This is demonstrated in Fig. 2, where the evolution of the lattice displacements is shown for representative realizations at 300 K in each of these cases. Notice the difference on the amplitude of the displacements in the linearized case (lower panel), comparing to the other two cases [28].

In Fig. 3, we plot the evolution of $\langle x^2(t) \rangle$ at different T for the cases (i) (dotted lines), (ii) (dashed lines), and (iii) (solid lines). Although the behavior of all three cases is similar in low T , where the weak thermal fluctuations are not able to explore the strongly nonlinear regime, this is not the case in the higher temperatures. In this high- T regime, there is a smooth crossover in the linearized case (iii) from $\sim t^2$ behavior at short times to $\sim t$ dependence at longer times, and the plateau disappears. On the contrary, the presence of hot spots at high T in the other two cases (i) and (ii) gives rise to anomalous behavior. Similarly, the same changes in [15] led to a disappearance of the increased charge's confinement with temperature only in the completely linearized case (iii), where there exist no breathers, contrasting the behavior exhibited in cases (i) and (ii) (see Fig. 3 of Ref. [15]). Therefore, it appears a consistent explanation that the anomalous diffusion, as demonstrated by the existence of sublinear diffusion and a plateau in $\langle x^2(t) \rangle$ at high T , is related to the existence of vibrational hot spots.

Plateaus in the evolution of the mean-squared displacement are typical signatures of caging effects observed in glassy systems. Charge diffusion in our coupled model exhibits similar anomalous behavior, like diffusion in other complex systems. However, there is a substantial difference between these two cases. In the case of glassy systems, the caging is due to mutual interactions between diffusive particles. The energy landscape experienced by a particular par-

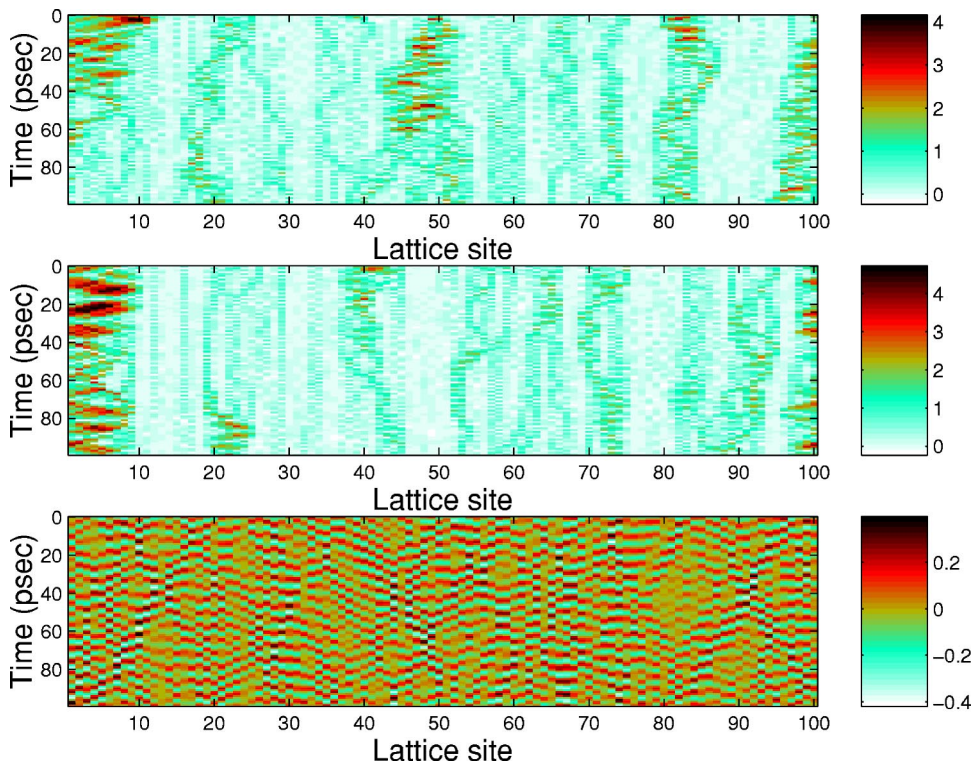


FIG. 2. (Color online) Density plots of the displacements from equilibrium, $y_n(t)$ (in Å), of each lattice site at $T=300$ K. A single thermal realization is shown for (i) the nonlinear lattice Hamiltonian (1) (upper panel), (ii) the case where $\rho=0$ in Eq. (1) (middle panel), and (iii) the completely linearized case where $\rho=0$ and the Morse potential has been substituted by its linearized form $M_{\text{lin}}(y_n) = Da^2 y_n^2$ (lower panel). Periodic boundary conditions have been used in a lattice consisting of 100 sites. The other parameters are the same as in Fig. 1. The bar at the right of each panel indicates the values represented by different color scales. The existence of hot-spots is evident in cases (i) and (ii).

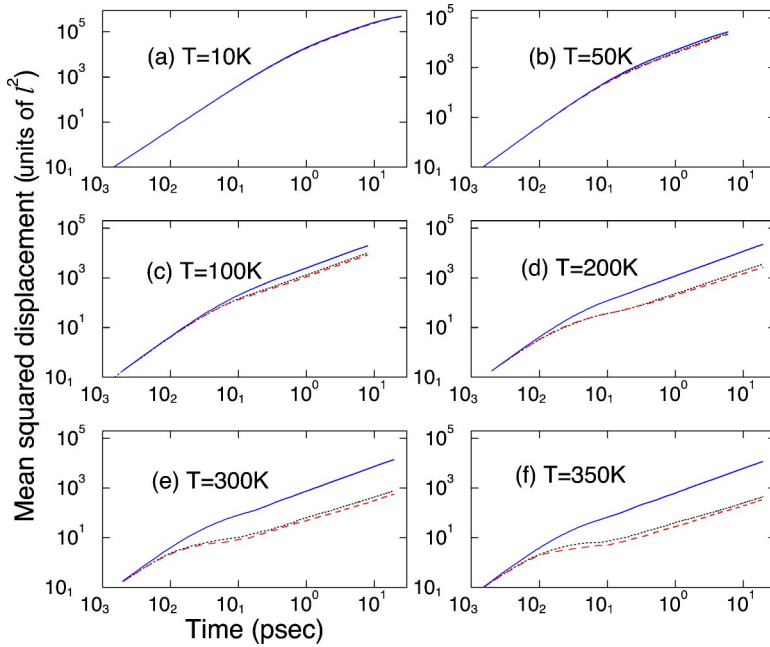


FIG. 3. (Color online) Time dependence of the mean-squared displacement $\langle x^2(t) \rangle$ (in units of squared lattice constant l^2), averaged over 200 thermal realizations, for (a) $T=10\text{ K}$, (b) $T=50\text{ K}$, (c) $T=100\text{ K}$, (d) $T=200\text{ K}$, (e) $T=300\text{ K}$, and (f) $T=350\text{ K}$. Dotted lines correspond to the full nonlinear lattice Hamiltonian, as in Fig. 1. Dashed lines correspond to $\rho=0$ in Eq. (1) (linear intersite interaction). Solid lines correspond to the completely linearized problem, i.e., $\rho=0$ and substituting the on-site potential $D(e^{-ay_n}-1)^2$ by its linearized form $Da^2y_n^2$ in Eq. (1). The other parameters are as in Fig. 1. The three cases cannot be distinguished at the lower temperatures.

ticle is fluctuating, since it is created from the nonlinear interactions with the neighboring particles, which also attempt to diffuse. Therefore, the anomalous relaxation results from motions in a fluctuating complex landscape, which is collectively created by the diffusive particles in question. In our case, the anomalous diffusive behavior is also due to a fluctuating landscape, but provided by an external field, viz., the vibrational hot spots of the anharmonic lattice dynamics (see Fig. 2), which act as temperature-dependent confinement potentials generating "cages" that hinder charge propagation. It is worth noticing at this point that complex dynamical behavior, typical of what is observed in glassy systems, has been also reported for the relaxation of the energy-energy correlation function in another breather bearing model (the one-dimensional ϕ^4 chain) [29].

Breathers at finite temperatures correspond to local deviations from thermal equilibrium, persisting for relatively long times (compared to characteristic vibrational times of the system). In the time scale of the diffusion observed in Figs. 1 and 3, this heterogeneity of the landscape at each individual case at high T is reflected by large deviations of individual trajectories from the averaged behavior. In Fig. 4, we plot the evolutions of $\sqrt{x^2(t)}$ [where $x^2(t)$ is given from Eq. (5)] for three random individual realizations (thin lines), and also the thermally averaged $\sqrt{\langle x^2(t) \rangle}$ (smooth thick lines), for different temperatures. Both cases of the fully anharmonic Hamiltonian (1) [case (i)] and the corresponding completely linearized problem [case (iii)] are shown for comparison. The significant degree of heterogeneity among individual trajec-

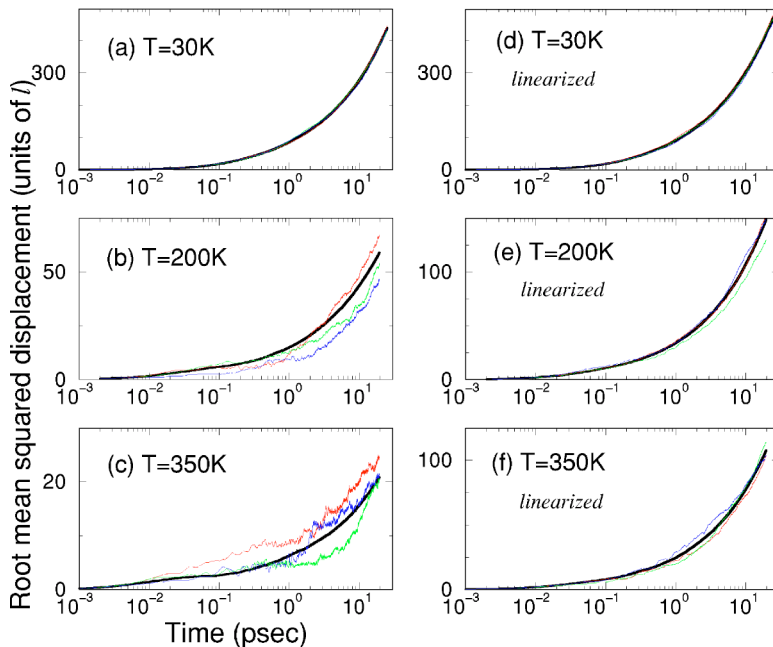


FIG. 4. (Color online) Time dependence of the root-mean-squared displacement (in units of lattice constant l) for three individual trajectories (thin lines), along with the thermal average obtained over 200 different realizations (smooth thick line), for temperatures (a),(d) 30 K , (b),(e) 200 K , and (c),(f) 350 K . (a), (b), and (c) correspond to the full nonlinear lattice Hamiltonian (1) [case (i)], while (d), (e), and (f) to the completely linearized problem [$\rho=0$ and linear on-site potential, case (iii)], respectively. The other parameters are as in Fig. 1. The individual trajectories are smooth and cannot be distinguished from the thermal average at the lower temperature.

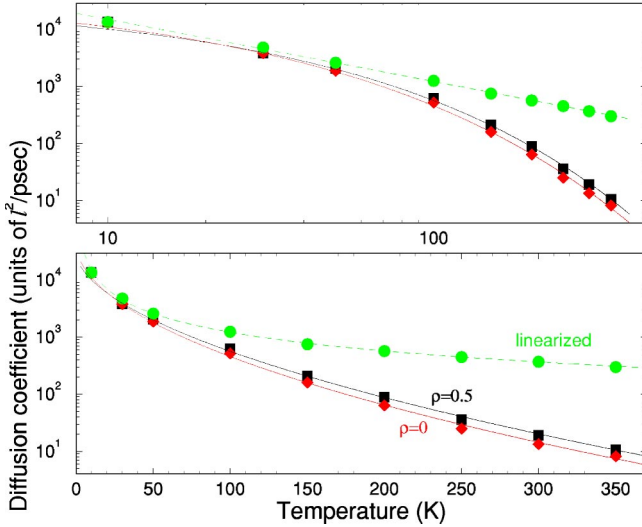


FIG. 5. (Color online) Diffusion coefficient (in units of l^2/ps , where l is the lattice constant) as a function of temperature in log-log scale (upper panel) and linear(X)-log(Y) scale (lower panel). Squares correspond to the full Hamiltonian (1), diamonds to linearized intersite interaction ($\rho=0$), and circles to the completely linearized lattice Hamiltonian ($\rho=0$ and substitution of the Morse potential by its linearized form). Continuous lines show fits of the former two cases with a stretched exponential law (7). The dashed line shows a fit of the completely linearized case with a power law (8).

tories, when hot spots are present, is evident in the plots. Case (ii) shows behavior similar to case (i).

IV. DIFFUSION COEFFICIENT

The above-discussed behavior has important effects on macroscopic transport parameters of the charge. At relatively high temperatures, hot spots lead to a suppression of the diffusion coefficient by one order of magnitude. This can be seen in Fig. 5, where the diffusion coefficient D is plotted as a function of temperature. We obtain D from the slope of the long-time linear dependence of $\langle x^2(t) \rangle$, as

$$\langle x^2 \rangle = 2Dt, \text{ for large } t. \quad (6)$$

In Fig. 5, we present the dependence of $D(T)$ for the three cases (i), (ii), and (iii) described in the previous section. In all cases D decreases with T , since larger thermal fluctuations hinder charge transport. However, the effect becomes more drastic when the lattice vibrations are anharmonic, where hot spots emerge. Then, at higher temperature, the density, size, and height of hot spots increase, and therefore more and stronger "cages" of smaller size appear impeding the charge's diffusion and decreasing the diffusion coefficient. A similar connection between slow dynamics and the topology of the energy landscape is known in glassy systems [30].

The variation of the diffusion coefficient with T in the nonlinear cases (i) and (ii) can be fitted by a stretched exponential formula,

$$D(T) = c \exp[-(T/T_0)^{\beta_s}]. \quad (7)$$

The fitted values for the case (i) (nonlinear intersite interactions, $\rho=0.5$) are $\beta_s=0.55$, $T_0=8$ K, and $c=3.1 \times 10^4 l^2/\text{ps}$, while for the case (ii) (linear intersite interactions, $\rho=0$) they are $\beta_s=0.51$, $T_0=5$ K, and $c=4.6 \times 10^4 l^2/\text{ps}$. The results of the fitting are shown in Fig. 5 with continuous lines.

On the contrary, the linearized case (iii) can be fitted well by a power law,

$$D(T) = \frac{c}{T^{\beta_p}} \quad (8)$$

(where T is given in K), with $\beta_p=1.09$ and $c=18.4 \times 10^4 l^2/\text{ps}$. This fit is also shown in Fig. 5 with dashed lines. The sum of the absolute values of the relative errors, $\sum |D_{\text{fit}} - D_{\text{calc}}|/D_{\text{calc}}$, is 8.6 for the power-law fit (8) of the linearized case and 20–25 for the stretched exponential fits (7) of the other two cases (with the main discrepancy in these cases coming from the lowest point at $T=10$ K). As can be seen from the log-log plots in Fig. 5 (upper panel), a power law cannot fit the nonlinear cases. Nonlinearity-induced hot spots result in a stronger temperature dependence of the diffusion coefficient.

We remind the reader here that without charge-lattice coupling (i.e., for $\chi=0$), the behavior of a tight-binding charge in one dimension cannot, in general, be diffusive [31]. In the absence of any disorder, the motion is ballistic, i.e., $x^2 \sim t^2$ [$= (2l^2 V^2 / \hbar^2) t^2$], due to the extended Bloch eigenstates. When static disorder is present, the localized nature of all the eigenstates results in a boundedness of x^2 ; in particular, $x^2(t)$ shows a transient diffusive behavior, but then it saturates approaching a localization length. In our case, Eq. (2), due to the coupling with the lattice fluctuations ($\chi \neq 0$), there is a dynamical disorder resulting in a diffusive motion at long times with a finite diffusion coefficient (at least for not so large values of χ).

V. NON-GAUSSIAN PARAMETER

The non-Gaussian parameter, given by

$$a_2(t) = \frac{\langle x^4 \rangle}{3\langle x^2 \rangle^2} - 1 \quad (9)$$

in one dimension, quantifies the deviation of the charge probability from a Gaussian shape [32]. In Fig. 6, we show the evolution of this parameter for the three cases (i), (ii), and (iii) for different temperatures. The results have been averaged over 200 thermal realizations. Again we see that at lower T the behavior of the wave function is similar in all three cases; it very quickly acquires a Gaussian shape and remains close to it during its evolution. However, the situation differentiates at higher temperatures. When nonlinearity and hot-spots are present [Figs. 6(a) and 6(b)], the deviations from a Gaussian become larger and very irregular due to the strongly fluctuating inhomogeneous landscape. On the contrary, in the linearized case the behavior remains qualitatively similar to that in lower temperatures, without any irregularities and strong deviations from a Gaussian shape.

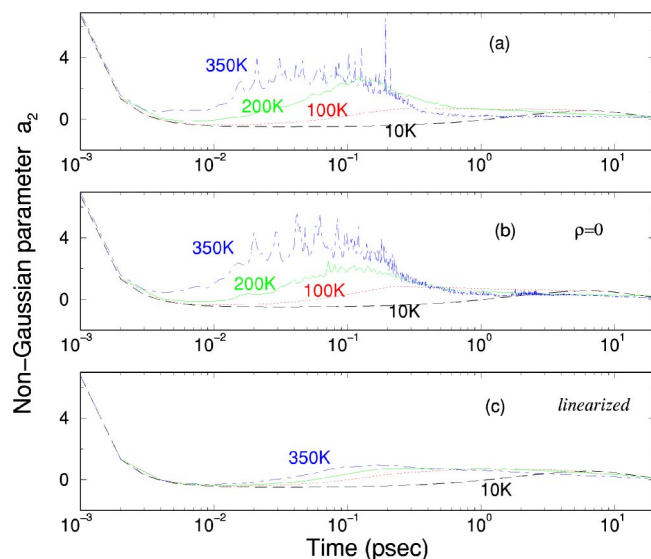


FIG. 6. (Color online) The non-Gaussian parameter a_2 as a function of time for (a) the full lattice Hamiltonian (1) [case (i)], (b) linearized intersite interactions [$\rho=0$, case (ii)], and (c) the completely linearized problem [case (iii)]. Dashed lines correspond to temperature 10 K, dotted to 100 K, solid to 200 K, and dot-dashed to 350 K. The other parameters are as in Fig. 1.

VI. DISCUSSION

Our calculations show features of anomalous diffusion in the propagation of a charge interacting with the fluctuating nonlinear dynamics of the underlying flexible lattice structure, at relatively high temperatures. The characteristics of this anomalous behavior are (a) existence of sublinear diffusion and a plateau in the mean-squared displacement, preceding the standard long-time diffusion, (b) heterogeneity among individual trajectories, and (c) a suppressed diffusion coefficient $D(T)$, having a stronger temperature dependence. These results demonstrate a similar phenomenology regarding charge transport in flexible materials at thermal equilibrium and complex behavior typically observed in glassy systems. We mention that similarities have also been found between relaxation properties of proteins and glasses [33].

Intrinsic inhomogeneous vibrational hot spots, spontaneously emerged by thermal fluctuations, are responsible for enhanced charge trapping on the microscopic level, related to the discussed anomalous phenomena. Anharmonic structural dynamics constitutes the key element for the presence of hot

spots. In the completely linearized vibrational system, the sublinear diffusion and the plateau disappear and the dependence of $D(T)$ can be described by a power law with exponent $\beta_p \approx -1$.

Nonlinear intersite interactions are not crucial in the model (1) for the presented anomalous behavior, since considering $\rho=0$ reproduces qualitatively similar results. Even though for the pure PBD lattice and its application to the DNA opening dynamics these intersite nonlinearities appear to be very important for the denaturation transition [23] and the correct positions of site-dependent openings in real DNA sequences at physiological temperatures [26], they have no significant effects in the case of charge transport coupled to the structure. This has been already suggested in previous studies [15]. Regarding charge motion, what seems to be important in the presence of charge-lattice interaction, at least in models similar to the Hamiltonian (1), is the on-site nonlinearity, which contributes the dominant effects.

Here we have an example where a particular property of a nonlinear system (macroscopic charge transport) could be possibly used to provide an indirect observation of breathers in thermal equilibrium. Up to now, studies of possible breather signatures in thermalized lattices have been mainly focused on spectral characteristics [34].

The phenomena discussed above are valid in the weak-coupling regime (small values of χ , i.e., existence of large polarons at $T=0$ K). They may be qualitatively different for relatively large coupling constants, where a single-site (small) polaron represents the ground state of the system at zero temperature. For example, in the case of a strongly localized polaron, it is expected that there exists a temperature regime where $D(T)$ increases with T , due to thermally activated hopping. The behavior in this regime is currently under investigation.

Finally, we expect that analogous anomalous properties of charge transport may be exhibited by other quasi-one-dimensional flexible systems, which are described through similar polaron Hamiltonians and characterized by strong nonlinearities in the structural dynamics at thermal equilibrium. It is an open question whether the observed behavior survives in higher dimensions, because of alternative escaping pathways available to the charge.

ACKNOWLEDGMENTS

We would like to thank P. Maniadis and S. Denysov for useful discussions.

[1] A. J. Heeger, *Angew. Chem., Int. Ed.* **40**, 2591 (2001).
 [2] C. Dekker and M. A. Ratner, *Phys. World* **August**, 29 (2001).
 [3] Y. A. Berlin, I. V. Kurnikov, D. Beratan, M. A. Ratner, and A. L. Burin, *Top. Curr. Chem.* **237**, 1 (2004).
 [4] R. G. Endres, D. L. Cox, and R. R. P. Singh, *Rev. Mod. Phys.* **76**, 195 (2004).
 [5] W. P. Su, J. R. Schrieffer, and A. J. Heeger, *Phys. Rev. B* **22**, 2099 (1980).

[6] A. R. Bishop, D. K. Campbell, P. S. Lomdahl, B. Horovitz, and S. R. Phillpot, *Synth. Met.* **9**, 223 (1984).
 [7] Z. G. Yu and X. Song, *Phys. Rev. Lett.* **86**, 6018 (2001).
 [8] R. Bruinsma, G. Grüner, M. R. D'Orsogna, and J. Rudnick, *Phys. Rev. Lett.* **85**, 4393 (2000).
 [9] A. J. Heeger, S. Kivelson, J. R. Schrieffer, and W. P. Su, *Rev. Mod. Phys.* **60**, 781 (1988).
 [10] E. M. Conwell and S. V. Rakhmanova, *Proc. Natl. Acad. Sci.*

- U.S.A. **97**, 4556 (2000); S. V. Rakhmanova and E. M. Conwell, *J. Phys. Chem. B* **105**, 2056 (2001).
- [11] D. M. Basko and E. M. Conwell, *Phys. Rev. E* **65**, 061902 (2002).
- [12] S. Komineas, G. Kalosakas, and A. R. Bishop, *Phys. Rev. E* **65**, 061905 (2002); P. Maniadis, G. Kalosakas, K. Ø. Rasmussen, and A. R. Bishop, *Phys. Rev. B* **68**, 174304 (2003).
- [13] D. Hennig, *Eur. Phys. J. B* **30**, 211 (2002); D. Hennig, J. F. R. Archilla, and J. Agarwal, *Physica D* **180**, 256 (2003).
- [14] G. Kalosakas, S. Aubry, and G. P. Tsironis, *Phys. Rev. B* **58**, 3094 (1998).
- [15] G. Kalosakas, K. Ø. Rasmussen, and A. R. Bishop, *J. Chem. Phys.* **118**, 3731 (2003); *Synth. Met.* **141**, 93 (2004).
- [16] S. Aubry, *Physica D* **103**, 201 (1997).
- [17] S. Flach and C. R. Willis, *Phys. Rep.* **295**, 181 (1998).
- [18] T. Dauxois, M. Peyrard, and A. R. Bishop, *Phys. Rev. E* **47**, 684 (1993); A. Bikaki, N. K. Voulgarakis, S. Aubry, and G. P. Tsironis, *ibid.* **59**, 1234 (1999); K. Ø. Rasmussen, S. Aubry, A. R. Bishop, and G. P. Tsironis, *Eur. Phys. J. B* **15**, 169 (2000); M. V. Ivanchenko, O. I. Kanakov, V. D. Shalfeev, and S. Flach, *Physica D* **198**, 120 (2004).
- [19] M. Peyrard and J. Farago, *Physica A* **288**, 199 (2000).
- [20] T. Pakula, *J. Chem. Phys.* **94**, 2104 (1991).
- [21] J. Habasaki, K. L. Ngai, and Y. Hiwatari, *Phys. Rev. E* **66**, 021205 (2002).
- [22] K. L. Ngai, *J. Phys.: Condens. Matter* **15**, S1107 (2003).
- [23] T. Dauxois, M. Peyrard, and A. R. Bishop, *Phys. Rev. E* **47**, R44 (1993).
- [24] A. Campa and A. Giansanti, *Phys. Rev. E* **58**, 3585 (1998).
- [25] C. H. Choi, G. Kalosakas, K. Ø. Rasmussen, M. Hiromura, A. Bishop, and A. Usheva, *Nucleic Acids Res.* **32**, 1584 (2004).
- [26] G. Kalosakas, K. Ø. Rasmussen, A. Bishop, C. H. Choi, and A. Usheva, *Europhys. Lett.* **68**, 127 (2004).
- [27] S. Chandrasekhar, *Rev. Mod. Phys.* **15**, 1 (1943).
- [28] The larger absolute values of negative displacements in the linearized case (iii) of Fig. 2, comparing to cases (i) and (ii), are due to the fact that the Morse potential is steeper than its linearized counterpart for values smaller than the equilibrium value.
- [29] S. Flach and G. Mutschke, *Phys. Rev. E* **49**, 5018 (1994).
- [30] S. Sastry, P. G. Debenedetti, and F. H. Stillinger, *Nature (London)* **393**, 554 (1998).
- [31] Apart from peculiar cases with singular continuous spectra.
- [32] A. Rahman, *Phys. Rev.* **136**, A405 (1964).
- [33] H. Frauenfelder, P. G. Wolynes, and R. H. Austin, *Rev. Mod. Phys.* **71**, S419 (1999).
- [34] M. Peyrard, *Physica D* **119**, 184 (1998); M. Eleftheriou, S. Flach, and G. P. Tsironis, *ibid.* **186**, 20 (2003); N. K. Voulgarakis, G. Kalosakas, K. Ø. Rasmussen, and A. R. Bishop, *Nano Lett.* **4**, 629 (2004).